Journal of Glaciology, Vol. 47, No. 156, 2001

Buoyancy-driven lacustrine calving, Glaciar Nef, Chilean Patagonia

Charles Warren,[1] Doug Benn,[1] Vanessa Winchester,[2] Stephan Harrison[3]
[1]*School of Geography and Geosciences, University of St Andrews, St Andrews, Fife KY16 9AL, Scotland*
[2]*School of Geography, University of Oxford, Oxford OX1 3TB, England*
[3]*Centre for Quaternary Science, Coventry University, Coventry CV1 5FB, England*

ABSTRACT. Glaciar Nef, a 164 km^2 eastern outlet of Hielo Patagónico Norte (the northern Patagonia icefield), terminates in a proglacial lake that has formed in conjunction with 20th-century glacier retreat. The terminus is inferred to be transiently afloat. A hinge-calving mechanism is proposed in which buoyant forces impose a torque on the glacier tongue, resulting in the release of coherent sections of the glacier tongue as "tabular" icebergs. A simple model shows how torque and tensile stress reach a maximum at the up-glacier limit of the buoyant zone, and that glacier thinning causes this point to migrate up-glacier. Empirical evidence supporting this model includes elevated thermo-erosional notches $\leq$6.5 m above lake level, and the ubiquitous presence since 1975 of "tabular" icebergs with surface areas $\leq$0.3 km^2. Flow speeds of 1.2–1.3 m d^{-1} were measured near the terminus in February 1998. Extrapolations from these short-term data yield a calving rate of 785–835 m a^{-1} and a calving flux of 232×10^6 m^3 a^{-1} or 0.2 km^3 a^{-1}. The calculated mean water depth at the terminus is 190 m. This calving rate is higher than at grounded temperate glaciers calving in fresh water, but is nevertheless almost an order of magnitude less than calving rates at both grounded and floating tidewater glaciers.

INTRODUCTION

Despite its obvious importance for the dynamics of many ice masses worldwide, calving remains a poorly understood process (Van der Veen, 1996). Of the three known categories of calving glacier — polar/floating, polar/grounded and temperate/grounded — the last is probably the best understood, as a consequence of detailed studies of tidewater glaciers in Alaska (Meier and Post, 1987; Powell, 1990, 1991; Meier, 1997; Van der Veen, 1997). Lacustrine calving, however, has received relatively little attention. Studies in Europe in connection with hydropower schemes (Funk and Röthlisberger, 1989; Hooke and others, 1989; Kennett and others, 1997) have shown that the well-established correlation between calving rates (u_c) and water depth (h_w) at tidewater glaciers in which u_c increases linearly with h_w (Brown and others, 1982; Pelto and Warren, 1991) also applies in lacustrine settings.

However, for any given depth of water, calving rates appear to be at least an order of magnitude less in fresh water than in tidewater. Explaining this surprising contrast is an important glaciological challenge (Meier, 1997; Hanson and Hooke, 2000) and has stimulated studies of the dynamics and glacio-climatic response of lacustrine calving glaciers in Greenland (Warren, 1991), New Zealand (Kirkbride and Warren, 1997, 1999) and Patagonia (Warren, 1994, 1999; Warren and others, 1995c; Naruse and others, 1997; Skvarca and Naruse, 1997; Harrison and Winchester, 1998; Rott and others, 1998; Naruse and Skvarca, 2000; Harrison and others, in press). These studies have confirmed the contrast in calving rates and proposed some preliminary process explanations. Although calving rates correlate positively with water depth, this may not be a causative correlation. The water-depth model has been challenged by Van der Veen and co-workers, who argue that terminus position is controlled by the ice thickness in excess of flotation (Van der Veen, 1996, 1997; Venteris and others, 1997; Venteris, 1999). The significance of the salinity of the proglacial water body has also been questioned using comparative data from Alaska and Patagonia (Venteris, 1999). A physical basis for the water-depth–calving-speed relation has been proposed by Hanson and Hooke (2000), who conclude that the influence of water depth on longitudinal deviatoric stresses near the terminus is one of many possible controls on calving speeds.

The primary aims of research carried out at Glaciar Nef, Patagonia, in February 1998 were to derive a calving rate, examine calving mechanisms and to chart the evolution of terminus geometry during historic glacier retreat. The results reported here contribute to the emerging regional dataset of calving statistics for Patagonia (Warren and Aniya, 1999). The building of such regional databases of calving-glacier statistics was one of several key recommendations of an international workshop on calving (Van der Veen, 1997) because "little progress can be made towards the goal of understanding calving processes without observational data" (Krimmel, 1997, p. 17). At present such data are limited.

GEOGRAPHICAL SETTING AND DESCRIPTION

Three mountain icefields with a total area of some 19 200 km^2 exist in southernmost South America (Warren and Aniya, 1999), nourished by the westerlies which deliver 6000–8000 mm a^{-1} of precipitation (Escobar and others, 1992; Rott and others, 1998). Although they remain poorly known (Warren and Sugden, 1993; Lliboutry, 1998), knowledge is

https://doi.org/10.3189/172756501781832403 Published online by Cambridge University Press

increasing rapidly, especially through the use of satellite imagery (Aniya and others, 1996; Aniya, 1999) and space-borne radar imagery (Rignot and others, 1996a, b; Forster and others, 1999; Michel and Rignot, 1999; Skvarca and others, 1999; Aniya and others, 2000). Since calving glaciers constitute a large and increasing majority of all outlet glaciers, icefield behaviour is inextricably linked with calving dynamics (Naruse and others, 1995a; Aniya and others, 2000), significantly complicating climatic and palaeoclimatic interpretations of glacier behaviour (Aniya, 1999; Luckman and Villalba, 2001). This has focused attention on calving dynamics (Naruse and others, 1995a, 1997; Warren and others, 1995a, b, 1997; Rott and others, 1998; Warren, in press).

Glaciar Nef (47°06′ S, 73°11′W) is one of eight major outlet glaciers which drain the eastern flank of Hielo Patagónico Norte (HPN; northern Patagonia icefield) (Fig. 1). The glacier has a surface area of 164 km^2 and is 33 km long, descending from its icefield accumulation area at 2800 m a.s.l. to a 1.4 km wide calving terminus in Lago Nef at 420 m a.s.l. (Aniya, 1988). The equilibrium line lies at around 1350 m a.s.l., indicating an accumulation-area ratio of 0.60 (Aniya, 1988). In 1975 the average surface gradient of the lower 10 km was 2° or 1:38. The northeastern side of the glacier currently consists of profusely crevassed clean ice (Fig. 2), but on its southwestern side, upstream of a large embayment, medial and lateral moraines merge to mantle the glacier with supra-

Fig. 2. The terminus of Glaciar Nef from the northeast, February 1998.

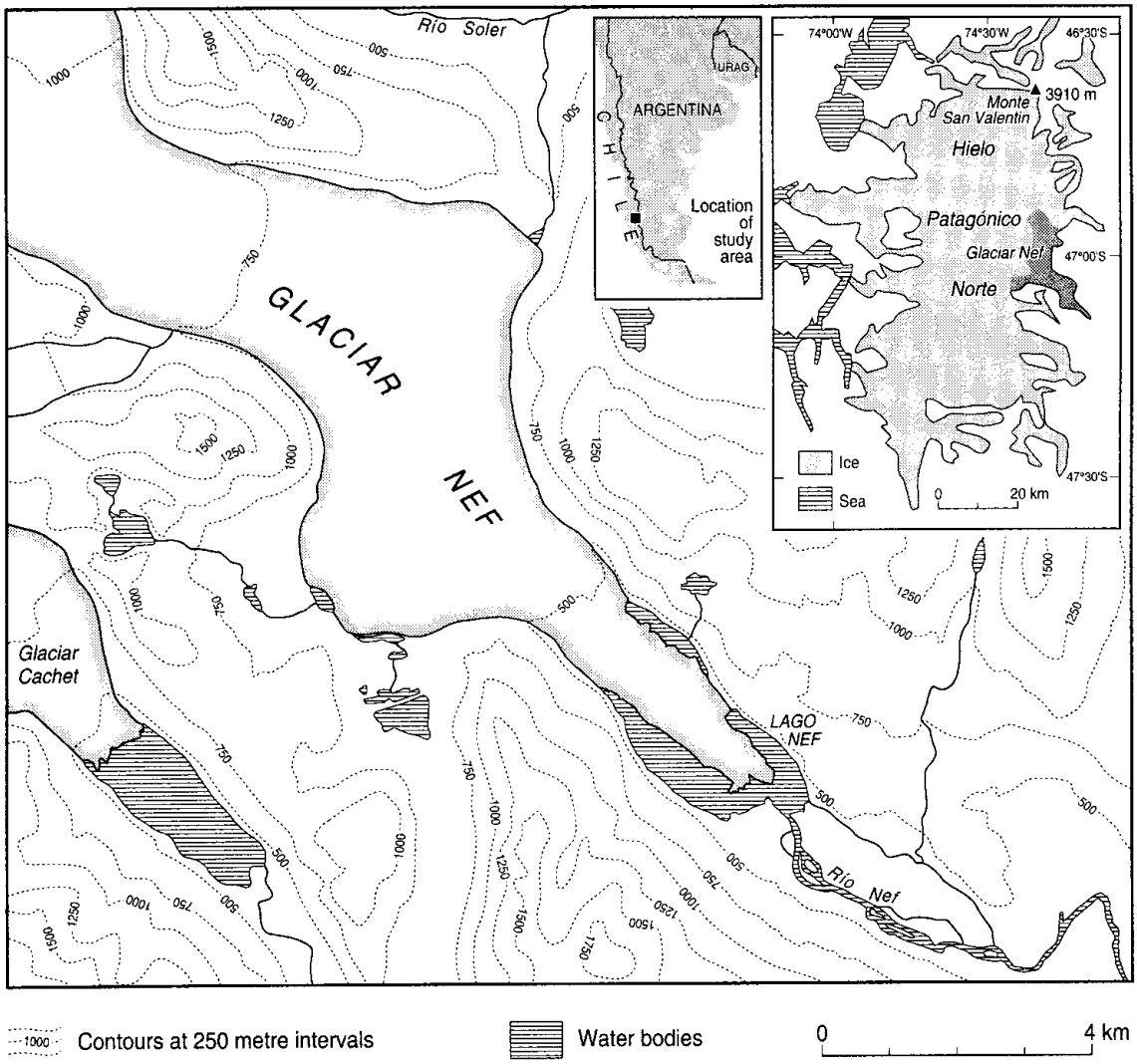

Fig. 1. The location of Glaciar Nef. The terminus is shown at its 1975 position. Simplified from 1:50 000 "Cordón Soler" sheet (Instituto Geográfico Militar de Chile). Insets: Hielo Patagónico Norte highlighting Glaciar Nef drainage basin (based on Aniya (1988)), and the location of HPN in South America.

https://doi.org/10.3189/172756501781832403 Published online by Cambridge University Press

glacial debris. This area derives from a tributary glacier whereas the calving terminus is sourced from the icefield. The calving front rises some 25–30 m above lake level at its centre, becoming lower towards both margins, and descending to water level at its northeastern end where, for a short distance, the ice margin parallels the shoreline and transverse crevasses form drowned re-entrants (Fig. 2). This configuration has changed little since November 1995 (personal communication from M. Aniya, 1997).

Previous work on the glacier is limited. Yoshida (1981) undertook preliminary geomorphological observations around Lago Nef, and Casassa (1987) reported a maximum ice thickness of 1000 ± 250 m in the upper part of Glaciar Nef. From a firn core obtained in the accumulation area, Matsuoka and Naruse (1999) derived accumulation and ablation values for 1996 of +5.6 and −3.4 m w.e., respectively, yielding a net balance of +2.2 m w.e. The only other work relating to the glacier has been low-level aerial observations of glacier-terminus change around HPN by Aniya and co-workers (Aniya and Enomoto, 1986; Aniya, 1992, 1999; Wada and Aniya, 1995; Aniya and Wakao, 1997) and analysis of change using RADARSAT and Landsat imagery (Aniya and others, 2000).

Glaciar Nef retreated during the 20th century, in common with the broad regional trend (Aniya and Enomoto, 1986; Aniya, 1999), and Lago Nef has formed and grown in conjunction with this retreat. Lichenometric evidence suggests that the terminus lost contact with its terminal moraine in the late 1930s (V. Winchester and others, unpublished data), and by 1944 a small arcuate ice-contact lake existed (Aniya and Enomoto, 1986). The lake is now some 4.5 km long and about 1.5 km wide. In February 1998 a profusion of icebergs choked almost the entire lake, with only small areas of open water at the northwest and southeast ends (Fig. 3). Prominent vegetation trimlines along the valley sides mark the 19th-century maximum (Fig. 3; Fig. 7, shown later), retreat from which is dated to about 1860 by lichenometry and dendrochronology (Winchester and others, in press). The southeastern end of the lake consists of a composite terminal moraine ridge some 500 m wide and rising ≤40 m above the lake. Río Nef, a tributary of Río Baker, at present begins at a prominent breach in this morainic rampart, but several large palaeo-channels cut across and skirt around the moraines. Some meltwater also drains northwards to the Río Soler down a side valley upglacier from the terminus (Fig. 1).

Fig. 3. Lago Nef and Glaciar Nef from the terminal moraines at the southeastern corner of the lake, February 1998. Note the 3 m long inflatable boat for scale. 19th-century vegetation trimlines are visible on the valley sides.

METHODS

Ice velocities

Surface ice velocities near the terminus were measured over an 8 day period (15–23 February 1998) with intermediate surveys on 17, 19 and 21 February. Displacement of prominent seracs was surveyed with an electronic distance meter (EDM)/theodolite from a 146 m baseline established on the southwestern (true right) valley side some 2.3 km from the glacier terminus (Fig. 4). Precipitous, unstable valley sides and the profusion of icebergs made closer approach impossible. The choice of the baseline and the seracs was dictated by the topography of the valley side and of the glacier surface.

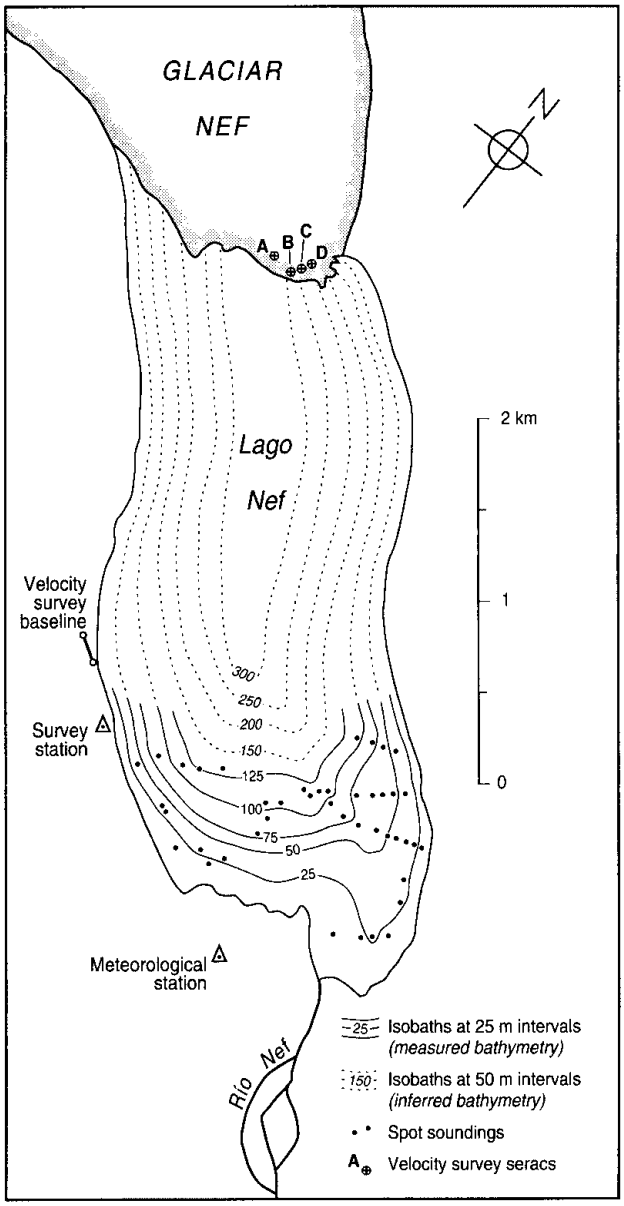

Fig. 4. Measured and inferred bathymetry of Lago Nef. Solid isobaths (25 m interval) indicate measured bathymetry, and dotted isobaths (50 m interval) represent inferred bathymetry (for explanation see text). Also shown are the seracs (A–D) on Glaciar Nef used for the velocity survey, the velocity survey baseline, the location of the survey station for the bathymetric survey, and the location of the meteorological station.

https://doi.org/10.3189/172756501781832403 Published online by Cambridge University Press

Bathymetry

Water depths in the southeastern third of the lake were measured with a Lowrance X-60 echo sounder with an instrumental accuracy of 3% of water depth, mounted on a small inflatable boat. Because icebergs prevented shore-to-shore transects, spot soundings were measured in all accessible open-water areas. The location of each sounding was surveyed with an EDM/theodolite sighting onto a prism in the boat from a survey station 58 m above lake level on the southwestern lateral moraines (Fig. 4).

Water temperatures

Five vertical water-temperature profiles were measured in the southeastern sector of the lake using an electronic water sensor with a maximum depth capability of 100 m that was designed and calibrated in the U.K. by the Institute of Freshwater Ecology. The temperature at each depth was averaged from down- and up-profiles. Laboratory calibration proves an accuracy of $\pm 0.02^{\circ}$C, but under field conditions an accuracy closer to $\pm 0.1^{\circ}$C is more likely.

Iceberg dimensions and meteorological observations

The heights and long axes of the largest icebergs were surveyed from the valley side. Subaqueous, near-surface geometry of icebergs near the southeastern end of the lake was investigated from the boat. Daily observations of air temperature (maximum and minimum), rainfall and sun hours were made at a station at the southeast end of Lago Nef (Fig. 4).

RESULTS

Characteristics of historic glacier retreat

The pattern of retreat of Glaciar Nef from the 19th-century maximum to 1998 is summarized in Figure 5. Two aspects are noteworthy. Firstly, retreat from the 1860s to the 1930s was slow despite significant surface lowering; 70 years after the onset of retreat the terminus was still in contact with part of the terminal moraine complex, and even as recently as 1984 the glacier was only 150 m from the moraine, a linear net retreat rate of just 3 m a^{-1} over the previous 50 years.

Secondly, from 1944 to 1984 the terminus narrowed by about 1000 m and thinned vertically by $\leq$90 m ($=$ 2.25 m a^{-1}) (Aniya and Enomoto, 1986), but the location of its front point changed little, even advancing a few tens of metres between 1975 and 1979. Even in the early 1990s when it was narrowing at $\leq$117 m a^{-1}, little retreat occurred (Wada and Aniya, 1995). Then, at some time between 29 December 1993 and 10 May 1994, the 2.25 km long tongue of ice calved and broke up in the lake (Wada and Aniya, 1995), fracturing along the line shown in Figure 5g. This event contributed significantly to the total area lost during 1987–97 of 2.07 km^2; in terms of percentage change to glacier surface area, this is the largest recent loss at any HPN glacier (Aniya and others, 2000). Just prior to its disintegration, the whole tongue drifted south a short distance (Aniya and others, 2000). The position of the northeastern glacier/rock junction remained almost unchanged between 1993 and 1998 while the terminus retreated 3.5 km at 875 m a^{-1}. Thus the dramatic onset of runaway recession in 1994 lagged the transition from a land-terminating to a calving terminus by 50–60 years.

Crevasse patterns, thermo-erosional notches and iceberg characteristics

During the 1944–94 period when the terminus consisted of a narrowing tongue, surface crevassing was dominantly longitudinal (Fig. 6). However, from 1975 all the vertical aerial photographs also show a narrow zone of transverse crevasses cutting the longitudinal set at 70–90° (Fig. 5). In all cases, the transverse crevasses exist either at -635 ± 35 m up-glacier from the terminus and/or at twice that distance up-glacier at -1300 ± 80 m. In the 1984 vertical aerial photograph and in a low-level oblique aerial photograph taken by the first author on 29 January 1991, the final few hundred metres of the glacier exhibit a reverse slope. In 1984 the transverse crevassing coincides with a zone in which the lateral ice margins are at lake level, down-glacier from which the ice surface rises towards a cliffed terminus.

In 1998, a set of horizontal thermo-erosional notches was present along the entirety of the 700 m long cliffed section of the glacier terminus (Fig. 7). The highest and most pronounced of these notches was 6.5 m above the waterline. One possible explanation for these would be a high lake stand. However, a recent 6.5 m rise of lake level would have left abundant evidence on the unconsolidated valley sides around Lago Nef, as well as downstream along the valley of Río Nef, but there was no evidence of lake stands greater than +0.5 m. The notches are therefore interpreted as having been formed at lake level by thermal erosion and subsequently raised to their observed position by buoyancy-driven upward displacement of the glacier terminus.

In combination, these observations of transverse crevassing, reverse slopes and elevated thermo-erosional notches suggest that the terminus of Glaciar Nef has been close to or at flotation (i.e. transiently afloat) since 1975. The preservation of these notches along 700 m of the terminus shows that large calving events are infrequent, and that even small-scale calving is rare between the large events. No calving was observed during the fieldwork in 1998.At least since 1975, calving has typically consisted of low-frequency, high-magnitude events. All the vertical aerial photographs show icebergs with long axes of several hundred metres (e.g. $\leq$460 m, 1979; $\leq$540 m, 1983) (Figs 5 and 6). In 1998, many of the large icebergs had long axes in excess of 300 m (maximum $=$ 600 m), surface areas of the order of 0.05–0.3 km^2, and were floating 30–50 m above water level. This is $\leq$20 m higher than the highest sections of the calving terminus. The preservation of the surface morphology of the lower glacier on many large icebergs (Fig. 8) demonstrates that they have calved without overturning. These characteristics are also apparent in 1995 oblique aerial photographs taken by M. Aniya. Several of the large icebergs were observed to drift, showing that they were free-floating, not grounded.

Despite surface water temperatures $<0.5^{\circ}$C, most of the icebergs at the southeast end of the lake possessed subaqueous shelves 0.2–1.0 m below the waterline and projecting as much as 25 m beyond their subaerial portions. These unusually extensive subaqueous projections are probably formed by the combination of intense insolation and very cold water, together with the effect of subaerial meltwater runoff.

Bathymetry

The measured and inferred bathymetry of Lago Nef is shown in Figure 4. Minimum estimates of water depth in the parts of

https://doi.org/10.3189/172756501781832403 Published online by Cambridge University Press

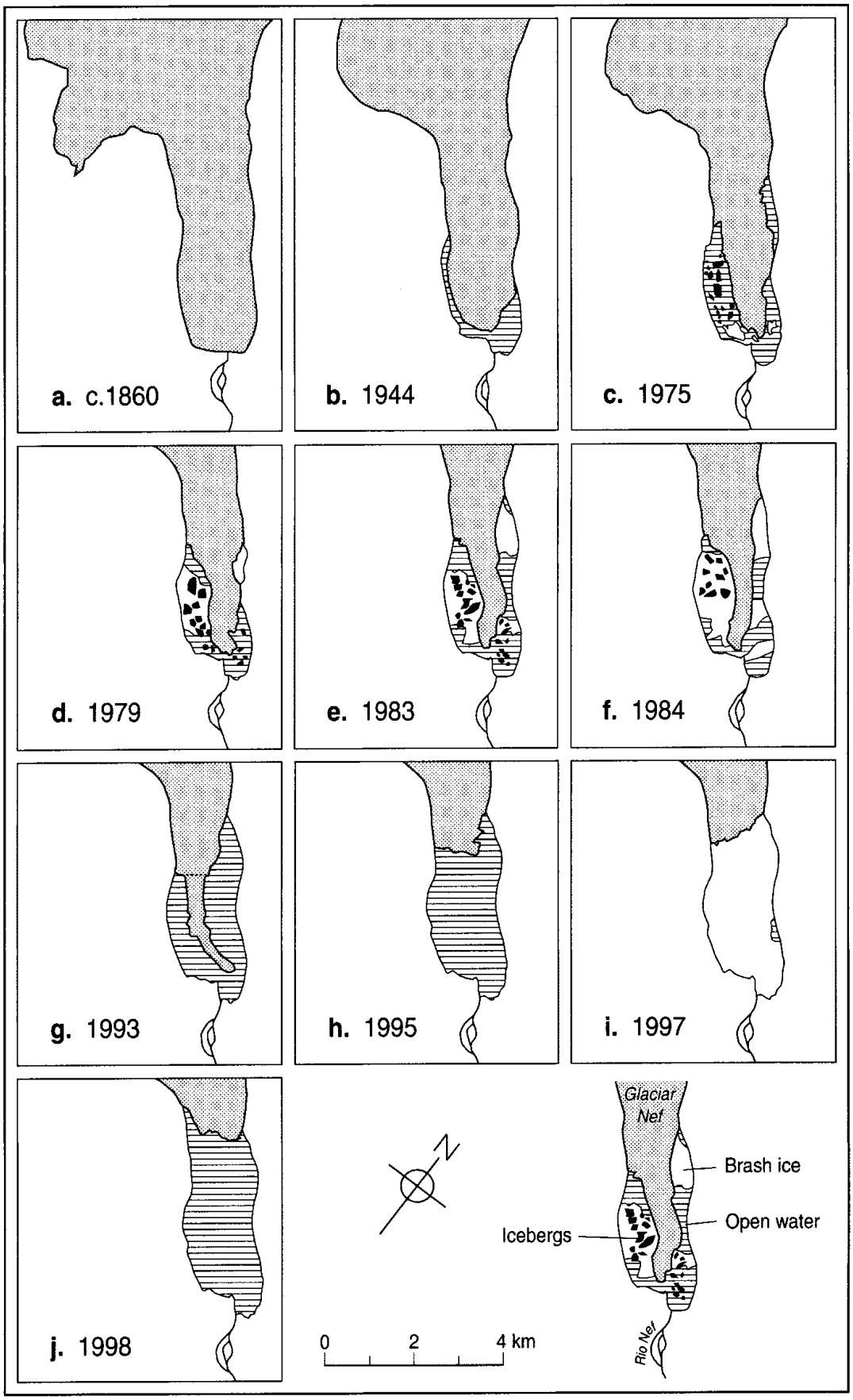

Fig. 5. Fluctuation history of Glaciar Nef from the mid-19th century to 1998. The 19th-century position is based on trimline evidence, and the date of about 1860 on lichenometric and dendrochronological data collected in 1998 (Winchester and others, in press). Icebergs, areas of brash ice and locations of transverse crevassing are shown only for the years with vertical aerial photographs; in 1997 almost the entire lake was choked with icebergs and brash ice, but the RADARSAT image does not permit icebergs to be resolved. The inferred transverse crevasse in panel h shows the line along which the tongue fractured between December 1993 and May 1994 (Wada and Aniya, 1995). Sources: vertical aerial photographs of November 1944, March 1975, March 1979, January 1983, March 1984; oblique aerial photographs of December 1993 (M. Aniya), November 1995 (M. Aniya); RADARSAT image of January 1997 (from Aniya and others, 2000); fieldwork in February 1998.

https://doi.org/10.3189/172756501781832403 Published online by Cambridge University Press

Fig. 6. Vertical aerial photograph of the lower part of Glaciar Nef in March 1979 (Instituto Geográfico Militar de Chile). Note the large icebergs and the dominantly longitudinal crevassing.

Fig. 7. Part of the calving terminus of Glaciar Nef, showing the highest thermo-erosional notch (arrowed) 6.5 m above the waterline. Note also the vegetation trimlines on the valley sides.

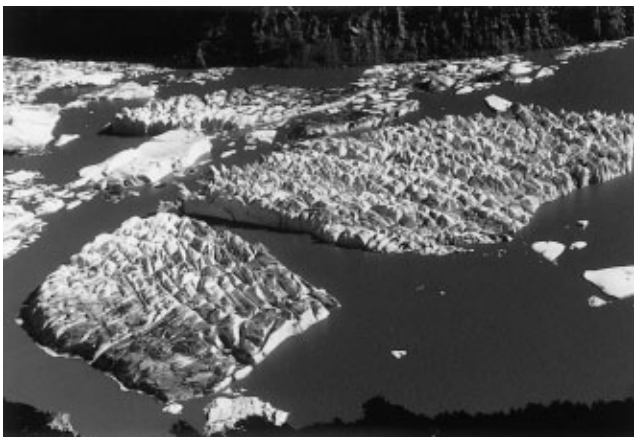

Fig. 8. Large "tabular" icebergs on Lago Nef, February 1998, showing the preservation of the surface morphology of the lower glacier.

Lago Nef that were inaccessible in 1998 can be inferred using two lines of evidence: the height of the glacier terminus, and estimates of the draughts of the largest icebergs.

If the glacier terminus is in hydrostatic equilibrium, the evidence for upward displacement of the terminus permits a calculation of the water depth (h_w) at the terminus. For hydrostatic equilibrium, the minimum water depth required for flotation is:

$$h_{wf} = 9h_0\,, \qquad (1a)$$

where h_0 is the thickness of ice above the waterline. Since, in the present case, the prominent thermo-erosional notch is 6.5 m above the present waterline, this must be the minimum depth of water beneath the ice, created by uplift. Thus,

$$h_w = 9h_0 + 6.5\,\text{m}\,. \qquad (1b)$$

For $h_0 = 25$ m, this yields a water depth of 231.5 m. High void ratios in greatly crevassed glaciers can reduce the height of the effective ice surface relative to that of mean visible (serac top) surface by several metres (Meier and others, 1994). Thus, the calculated water depth should be regarded as a maximum. Note that the glacier margin could have been in hydrostatic equilibrium both at the time the thermo-erosional notch was cut *and* at the time of observation, if uplift was driven by surface ice ablation.

However, the fact that the upper surfaces of several of the large, free-floating "tabular" icebergs are at a height $\leq$20 m above the glacier terminus indicates that it is not in hydrostatic equilibrium and that, upon release, the icebergs rise to achieve equilibrium. If so, Equation (1b) underestimates h_w. The wide distribution of large, non-grounded icebergs in the lake indicates that it is steep-sided with a substantial area of deep water. Taking account of void space, the geometry and surface heights of the icebergs suggest that parts of the lake must be >300 m deep. In support of this inference, ice-thickness data from 1985 (Casassa, 1987) indicate a maximum water depth close to the present terminus of 307 m. For testing the correlation between calving speed and water depth, the crucial information is the width-averaged water depth at the glacier terminus. Figure 4, constructed using the above inferences, suggests that the mean water depth at the calving front is 190 m.

Water temperatures

Water temperatures were low and varied insignificantly, either spatially, temporally or with depth. This is unsurprising in a lake dominated by floating ice. The southeast end of the lake was essentially isothermal. Maximum and minimum recorded temperatures were 0.48° and 0.28°C, respectively, and even during windless, sunny days the surface temperature rose by <0.1°C. Thin lake ice formed most nights and melted by mid-morning.

Ice velocities

Ice-velocity data are given in Table 1. Results were obtained from only four points due to the limited number of distinctive seracs with flow vectors that were suitably oriented with respect to the baseline. Ice velocities for the southwestern

Table 1. Displacements of seracs near the terminus of Glaciar Nef, 15–23 February 1998. Locations of seracs are shown in Figure 4

Serac	Survey period		Displacement	Velocity	
	Interval	Number of hours			
			m	m d^{-1}	m a^{-1}
A	19–23 Feb.	95	4.6	1.16	418
B	17–23 Feb.	144	7.07	1.18	430
C	15–23 Feb.	189	9.94	1.26	460
D	15–23 Feb.	189	8.91	1.13	413

https://doi.org/10.3189/172756501781832403 Published online by Cambridge University Press

part of the terminus could not be determined, because ice flow in this area was towards the baseline. Some of the early intermediate surveys of seracs A and B yielded spurious results, so data for later periods were used. Extrapolations to annual values are given to facilitate comparison with other calving data which are conventionally expressed as annual figures. There is evidence that seasonal variability in flow speed in Patagonia is limited (cf. discussion in Warren (1999)), and thus that extrapolations from seasonal to annual values can be meaningful. Nevertheless, given the short measurement period, these data permit only the provisional estimate that the width-averaged flow speed close to the terminus is of the order of 0.8–1.0 m d^{-1} or 300–350 m a^{-1}.

Meteorological observations: the 1997/98 El Niño

One of the strongest El Niño events in recent decades peaked in February 1998. It affected Patagonia to an unusual extent due to a Southern Oceans anticyclone that was anomalously intense and east-shifted relative to previous large El Niño–Southern Oscillation (ENSO) events (Winchester and others, 1999). The sustained calm, sunny conditions which resulted may have contributed to the minimal calving activity. Mean daily maximum and minimum temperatures were 17° and 4.5°C, respectively.

DISCUSSION

Characteristics of glacier retreat

During the 20th century, most HPN outlet glaciers have retreated, coincident with a warming of 0.4–1.4°C south of latitude 46° S since the beginning of the century (Rosenblüth and others, 1995). In the period 1944–96, HPN lost 1% of its surface area (Aniya, 1999). However, the rates and timings of glacier recession have been rather variable (Aniya and Enomoto, 1986; Aniya, 1999). In particular, an east–west contrast is apparent in the historic and current behaviour of many of the outlet glaciers (Aniya, 1988; Warren and Sugden, 1993). Recession generally accelerated during the 1970s and 1980s (Lliboutry, 1998), but during the 1990s retreat rates of most glaciers decreased, with several achieving stability or readvancing small distances. This probably reflects a delayed response to a marked precipitation increase from the 1970s (Winchester and Harrison, 1996; Harrison and Winchester, 1998; Aniya, 1999). However, four lacustrine calving glaciers (Reicher, Gualas, Steffen, Nef) experienced accelerated retreat in the 1990s as narrowing termini calved and/or broke up in ice-contact lakes (Wada and Aniya, 1995; Aniya and Wakao, 1997). Since 1990 the climatically-driven trend seems to have been towards more positive mass balances, with some dynamically induced noise superimposed (e.g. calving; debris cover). As suggested by Aniya (1999), the rapid calving retreats during the 1990s are most probably delayed responses to negative mass balance during earlier decades.

The geometry of the recent retreat at Glaciar Nef is noteworthy for two reasons. Firstly, a pattern of terminus narrowing and downwasting followed by rapid recession seems to be characteristic of lake-calving glaciers following the non-calving/calving transition. In recent decades, for example, such a pattern has been observed at lacustrine glaciers in Norway (Theakstone, 1989), Patagonia (Warren, 1994; Aniya, 1999) and New Zealand (Kirkbride, 1993; Hochstein and others, 1998). The formation of long, narrow tongues of this kind is not, however, known to occur at tidewater glaciers. This concurs with previous work which concluded that lacustrine glaciers are inherently more stable than tidewater glaciers (Warren, 1991). Secondly, the unchanging position of the northeastern glacier/rock junction while the terminus retreated >3.5 km in pivotal fashion during the 1990s is an interesting example of the role of topographic pinning points (cf. Mercer, 1961; Warren, 1991) in the stability and evolution of calving termini.

Buoyancy-driven calving

Evidence and interpretation

Calving at Glaciar Nef consists of high-magnitude, low-frequency events, producing some of the largest icebergs in Patagonia. Four lines of evidence demonstrate the importance of buoyant forces at this site since 1975:

- thermo-erosional notches ≤6.5 m above lake level, indicating upward displacement of the glacier terminus.
- transverse crevasses cutting the narrow ice tongues of the 1970s and 1980s; in 1984 and 1991 these are coincident with a transition from normal to reverse slopes.
- the ubiquitous presence of large "tabular" icebergs floating ≤20 m above the terminus and in their original orientation (i.e. not having overturned). The vertical aerial photographs and observations by Aniya in 1995 show that this has been typical at least since 1975 (cf. Fig. 6).
- the southward drift of the narrow glacier tongue just prior to its disintegration early in 1994 is interpreted by Aniya and others (2000) as being indicative of flotation.

What combination of processes and factors simultaneously inhibits "normal" calving (with the production of prismatic icebergs) while promoting buoyancy-driven calving (with the production of "tabular" icebergs)? Two primary candidates are:

- rapid thinning combined with slow terminus retreat progressively reducing the surface gradient until buoyant uplift of the glacier tongue occurs.
- ice near the terminus approaching flotation, causing basal shear stress to decrease to zero.

Aerial photographs show that open transverse crevasses are absent from most of the lower part of the glacier, indicating that the glacier terminus is not undergoing longitudinal extension. This will inhibit small-scale calving, especially given near-freezing water temperatures which will result in low rates of waterline and subaqueous melting (cf. Kirkbride and Warren, 1997). In the absence of tidal flexure and wave action, both of which can promote calving in tidewater settings, surface melting becomes the dominant ablation process. Limited data on ablation rates and ice-thickness change on eastern outlet glaciers of the Patagonian icefields suggest that Glaciar Nef could lose 4–11 m a^{-1} of ice thickness close to the terminus (Kobayashi and Saito, 1985; Naruse and others, 1995a, b, 1997). We suggest that it is surface ice loss which causes large, coherent sections of the tongue to reach flotation, creating an upward bending moment which causes calving.

A model of buoyant calving

The principle of buoyancy-driven calving is illustrated and tested in a simple model of a water-terminating glacier

https://doi.org/10.3189/172756501781832403 Published online by Cambridge University Press

tongue (Fig. 9a). The ice terminates in water with depth h_w, rests on a horizontal bed and has a constant gradient α. We assume that longitudinal stresses are negligible. The ice thickness required for flotation is:

$$h_n = (\rho_w/\rho_i)h_w\,, \tag{2}$$

where ρ_w and ρ_i are the densities of water and ice, respectively. The ice tongue will be buoyant where the ice thickness, h_i, is less than h_n. The magnitude of the buoyant force is found from:

$$\sigma_z = \rho_i g(h_i - h_n)\,, \tag{3}$$

where g is gravitational acceleration. σ_z is positive downwards, and negative σ_z corresponds to buoyant ice. Buoyancy produces a torque in the ice, and at a distance x_i from the ice margin the torque (bending moment) is given by:

$$M = \int_0^i \sigma_z x\,\mathrm{d}x\,. \tag{4}$$

The torque acts around a horizontal neutral axis located at $y = 0.5h_i$ and results in compressive stresses in the x direction above the neutral axis, and corresponding tensile stresses below the neutral axis, rising to a maximum at the ice base (Fig. 9b). The tensile stresses are opposed by cryostatic pressure, and the tensile stress at the ice base is given by:

$$\sigma_{x\max} = (0.5h_i M)/I \tag{5}$$

(positive $\sigma_{x\max}$ = compressive; negative $\sigma_{x\max}$ = tensile). I is the moment of inertia, and is related to the shape of the cross-section. For a rectangular cross-section of unit width,

$$I = (h_i^3)/12\,. \tag{6}$$

For an ice tongue with an initial terminal thickness h_n, surface ablation will result in the formation of a buoyant marginal zone, which will lengthen as the ice progressively thins. The torque and $\sigma_{x\max}$ produced by the buoyant ice are at a maximum at the up-glacier limit of the buoyant zone, where $h_i = h_n$. Figure 10 shows calculated values of $\sigma_{x\max}$ for $\alpha = 5^\circ$ and $\alpha = 2^\circ$, for a range of terminal ice thicknesses. As ice thickness decreases, the basal tensile stress increases, and the point of greatest tensile stress migrates up-glacier. For a given terminal ice thickness, basal tensile stresses are greater for $\alpha = 2^\circ$ than $\alpha = 5^\circ$ because low-gradient ice tongues can become buoyant over a greater length of the snout.

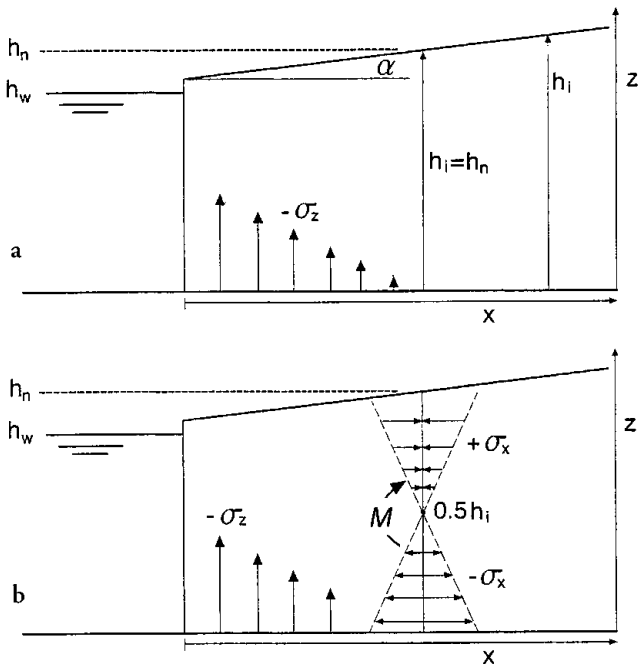

Fig. 10. Basal tensile stresses resulting from buoyant forces for a range of terminus ice thicknesses and surface gradients of 5° and 2°. The calculated stresses are based on the assumption that the ice remains in contact with the bed, and that buoyant forces are unresolved by upwarping of the ice. Upwarping rates will increase, and fracture becomes increasingly likely as the length of the buoyant zone increases. Fracture will be encouraged by high ablation rates.

The evolution of basal tensile stresses with decreasing ice

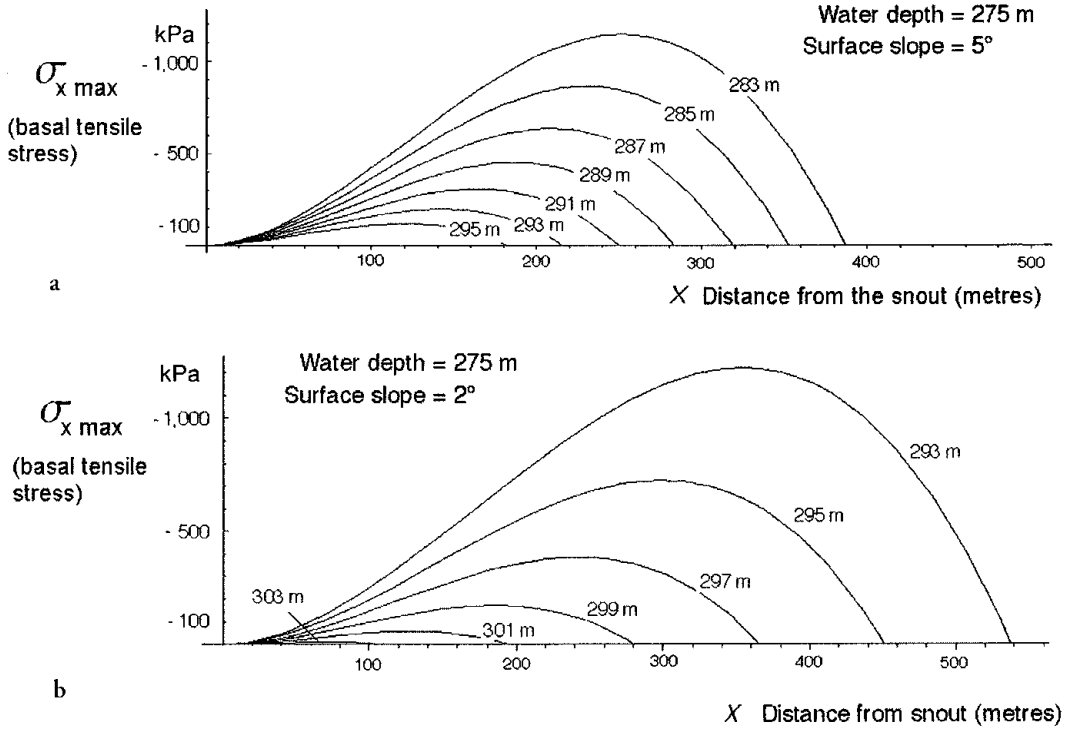

Fig. 9. (a) Definition sketch of an ice tongue with a buoyant margin. (b) Development of torque (M) and longitudinal stresses σ_x arising from the buoyant forces.

https://doi.org/10.3189/172756501781832403 Published online by Cambridge University Press

thickness shown in Figure 10 assumes that the position of the ice base does not change through time, and that buoyant forces are unresolved by ice creep. However, upward bending of the ice will occur in response to the torque imposed by the buoyant forces, due to longitudinal extension and thinning below $0.5h_i$ and longitudinal shortening and thickening above h_i. Upward bending will reduce the buoyant forces acting on the ice tongue, and thus, at any point in time, the tensile stresses at the ice base will arise from the remaining buoyant forces unresolved by creep. Brittle failure will occur at the base of the ice when $\sigma_{x\max}$ exceeds the tensile strength of the ice: $\sigma_{x\max} > \sigma_{\text{crit}}$. Since $\sigma_{x\max}$ occurs at the base of the ice, failure will commence at the glacier bed and propagate upwards. Failure is likely to be catastrophic, because fracture growth reduces the local ice thickness h_i, thus reducing the moment of inertia I, and increasing the tensile stress at the fracture tip (Equation (5)).

The tensile strength of glacier ice has been determined experimentally by Gagnon and Gammon (1995), who showed that for intact ice close to the pressure-melting point, tensile strength is about 1 MPa. Lower values (about 0.1–0.2 MPa) were calculated by Vaughan (1993) from the occurrence of crevasses on temperate glaciers, although these values relate to low-density near-surface firn rather than deep ice. Taking a value of 1 MPa as an upper limit, the model predicts that, in the absence of ice creep, buoyancy-driven fracture will occur on low-gradient glaciers at distances of 200–400 m from the terminus, depending on ice surface gradient. Despite the idealized nature of the model, it is interesting to note that during the last 25 years, while the glacier's surface gradient has been $\leq 2^\circ$, icebergs have typically had dimensions of several hundred metres.

Determining rates of ice creep and upward bending for given ablation rates and ice geometries is beyond the scope of this paper. However, as a general point, it can be said that ice creep is more likely to fully accommodate evolving buoyant forces when ablation rates are low, and that unresolved tensile stresses are more likely to exceed the tensile strength of ice when ablation rates are high. Thus, for a buoyant ice tongue, upward bending of the snout is more likely to occur during the winter months, and fracture of the buoyant portion is more likely to occur in summer when ablation rates are high.

Adopting aspects of the model of Lingle and others (1993), the observations at Glaciar Nef in 1998 are suggestive of a three-stage response of the glacier as the terminus accommodates the increasing buoyancy-driven torque:

1. In the initial stage, when terminal ice is slightly less than h_n, the buoyant zone is confined to a small portion at the end of the tongue. Because the torque and basal tensile stresses are small, ice-creep rates are low, and the buoyant terminal ice is held below hydrostatic equilibrium by the non-buoyant ice upstream. Thermal erosion at the waterline forms a notch.
2. During the second stage, glacier thinning by surface ablation causes the limit of the buoyant zone to migrate up-glacier. Torque increases and the terminus begins to upwarp, lifting the thermo-erosional notch above lake level.
3. The final stage involves catastrophic failure, either at the point of maximum moment (the up-glacier limit of the buoyant zone) or at a point where bottom topography introduces a local stress concentration. The entire terminal zone down-glacier of this point is then released as one or more icebergs. If the terminus does not achieve hydrostatic equilibrium through up-warping prior to calving, these icebergs will float higher than the glacier terminus.

The existence of multiple thermo-erosional notches demonstrates that the up-warping of the terminus is not instantaneous upon reaching flotation, but occurs progressively. In the late 1970s and 1980s, the up-glacier limit of the buoyant zone (inferred from the transverse crevassing) was located about 635 ± 35 m up-glacier from the terminus. Icebergs with long axes $\leq$600 m were present in Lago Nef in both November 1995 and February 1998, suggesting that even with a very different glacier-terminus geometry (cf. Fig. 5) the point of maximum moment may still be located approximately the same distance up-glacier of the calving front.

Comparison with previous observations

A role for buoyant forces in triggering lacustrine calving has previously been suggested from observations in Alaska (Lingle and others, 1993), Norway (Theakstone and Knudsen, 1986; Theakstone, 1989), Arctic Canada (Holdsworth, 1973) and in Iceland by Howarth and Price (1969) who propose a buoyancy-driven hinge-calving mechanism from work at Breiðamerkurjökull. At the same site, Derbyshire (1974) infers that sections of the terminus are close to or at flotation, and presents photographic evidence (plate IVb) showing many of the features reported at Glaciar Nef (e.g. large, flat-topped icebergs floating significantly higher than the terminal ice cliff). Additionally, the terminus zone exhibits a reverse slope, increasing in height from the base of an icefall a short distance up-glacier. This situation is also reported at Austerdalsisen, Norway, by Theakstone (1989).

Most pertinently, buoyant forces are invoked by Lingle and others (1993) in their proposal of an "inverse Reeh" calving mechanism (cf. Reeh, 1968) from observations at Bering Glacier. Prior to the arrival of the 1993 surge front, the terminus in Vitus Lake was held below hydrostatic equilibrium by the tensile strength of the uncrevassed ice; due to this positive buoyancy, icebergs which calved from the low calving cliff "popped up" and floated substantially higher than the general level of the terminus. "Normal" calving was apparently inhibited by the absence of crevasse-forming deformation during the 28 year quiescent period. Upon the arrival of the surge front in 1994, profuse, large-scale calving immediately ensued as substantial areas became afloat and broke up (personal communication from A. Post, 1995).

Powell (1990) and Alley (1991) argue that temperate glaciers cannot form floating ice shelves because abundant englacial and inter-crystalline water makes the ice too weak to resist calving in the absence of restraint from basal shear stress. The evidence reported here and in the studies cited above indicates that they can, albeit only locally and briefly. Lliboutry (1998) also infers periods of terminus flotation of several Patagonian glaciers from their 20th-century oscillations, and A. Post (personal communication, 1995) cites examples of temperate glacier tongues floating in lakes in Alaska. He stresses, however, that they can only survive when lateral or bottom topography provides stability; when they become free-floating they break up rapidly.

It has also been argued by Van der Veen and co-workers (Van der Veen, 1996, 1997; Venteris and others, 1997; Venteris, 1999) that once a calving glacier terminus thins below a flotation criterion (suggested to be about 50 m in excess of flotation) rapid calving ensues until the terminus has

https://doi.org/10.3189/172756501781832403 Published online by Cambridge University Press

retreated to a position where its thickness exceeds flotation. It seems that this threshold is indeed significant for many calving glaciers. Equally, however, it is clear from this study and the observations of buoyant calving cited above that some glaciers thin beyond the flotation criterion without undergoing rapid calving retreat. At such glaciers, the key threshold is not 50 m in excess of flotation, but flotation itself. An important but unanswered question arises: what determines which of these two thresholds controls calving behaviour? It may well be significant that all the glaciers at which calving has been linked to buoyancy-induced stresses calve into lakes, not into tidewater. Longitudinal strain rates (or their absence) are also likely to be a significant factor.

Several studies have noted that the size/frequency distribution of icebergs produced by lacustrine calving is typically distinct from that in tidewater, with the former producing a higher percentage of large icebergs than the latter (Qamar, 1988; Warren, 1991; Kirkbride, 1993). Glaciar Nef represents an end member of this spectrum, with very large icebergs produced by hinge calving. Large, flat-topped icebergs have also been noted in ice-contact lakes in front of slow-flowing, debris-mantled glaciers (e.g. Miller Lake, Alaska (Reid and Callender, 1965); Hooker Lake, New Zealand (Warren and Kirkbride, 1998)), but these have been interpreted as the products of subaqueous calving from a submerged "ice foot" of the kind inferred by Kirkbride and Warren (1997) and described by Hunter and Powell (1998).

Calving rates

Tidewater vs fresh water

Mean calving rate (u_c in m a^{-1}) can be obtained from the equation:

$$u = u_i - u_c \,, \tag{7}$$

where calving rate, u_c, is related to the rate of terminus change, u, and ice velocity, u_i, both averaged over the terminus width. Taking u_i to be 300–350 m a^{-1}, and u (January 1997–February 1998) to be −485 m a^{-1}, Equation (7) yields a calving speed of 785–835 m a^{-1}. This estimate does not incorporate melt rates along the calving face of Glaciar Nef. These are unknown, but are likely to be small (<20 m a^{-1}) relative to u_c, especially given water temperatures <0.5°C.

The standard form in which the u_c/h_w relationship is expressed is

$$u_c[\mathrm{m\,a^{-1}}] = k[\mathrm{a^{-1}}]h_w \,, \tag{8}$$

where k is an empirical constant. For temperate tidewater glaciers in Alaska, $k = 27.1 \pm 2$ a^{-1} (Brown and others, 1982). The recent behaviour of Glaciar Nef is consistent with $k = 4.3$. Combining the ice-cliff height with a mean water depth of 190 m, the mean ice thickness at the calving front is taken to be 205 m. Given that $u_i = 300$–350 m a^{-1} and that the glacier is 1400 m wide, this yields an annual mass flux at the terminus of approximately $86–100 \times 10^6$ m^3 a^{-1}. If $u_c =$ 810 m a^{-1}, the annual calving flux is about 232×10^6 m^3 a^{-1} or 0.2 km^3 a^{-1}. Given that h_w is likely to be >190 m, these are minimum estimates.

These figures are approximate, but all of them indicate that the calving speed at Glaciar Nef is far below typical tidewater rates. For h_w = 190 m, the tidewater value of k predicts a calving speed of 5150 m a^{-1}, more than six times greater than the calculated calving rate. If h_w is in fact >250 m, a calving speed >6750 m a^{-1} would be expected in tidewater, eight times faster than the calculated rate. These data thus strengthen the growing consensus that calving rates in fresh water are almost an order of magnitude less than in an equivalent depth of tidewater. Further, they indicate that even in deep lakes where the glacier terminus is intensely crevassed and reaches flotation, calving rates are still many times slower than tidewater calving speeds, despite the fact that they exceed typical rates for lacustrine calving.

Grounded vs floating

For grounded lake-calving glaciers, Funk and Röthlisberger (1989) and Warren and others (1995c) derived best estimates of $k = 1.9 + 12$ m a^{-1} and $k = 2.5 \pm 0.5$ m a^{-1}, respectively. The fact that $k = 4.3$ at Glaciar Nef is unsurprising given that buoyancy-driven hinge calving and grounded calving are different processes. It is unreasonable to apply a u_c/h_w relationship to a floating calving terminus, as it would imply that u_c increases with increasing h_w below the floating tongue. This is most improbable, unless basal melt rates are progressively enhanced, in turn accelerating calving in some way.

Although the value of k at Glaciar Nef is higher than that found in studies of lacustrine calving at grounded termini, it is nevertheless broadly compatible with such studies. Given the transiently floating condition of Glaciar Nef, this is curious, but it is consistent with Pelto and Warren's (1991) study which found that u_c correlated with h_w at both grounded and floating termini. It is likely that glacier thickness (h_i) rather than h_w explains this apparent anomaly because calving studies have consistently found strong correlations between u_c, on the one hand, and both h_w and h_i on the other (Brown and others, 1982; Reeh, 1994). This highlights the difficulty of identifying the dependent and independent variables in the calving problem (cf. Venteris, 1999), and the perennial danger of interpreting correlation as causation.

CONCLUSIONS

The key findings of this work are:

1. Imbalanced hydrostatic stresses at calving termini which reach flotation impose an upward-bending moment which leads to infrequent but high-magnitude hinge calving. At Glaciar Nef, such buoyancy-driven calving has been significant at least since 1975, and appears to have become dominant since 1994.

2. Glaciar Nef flows at about 300–350 m a^{-1} and calves at some 785–835 m a^{-1} in a mean water depth ≥190 m. Much of Lago Nef is probably >200 m deep, and water temperatures are close to freezing. These results support existing data which indicate that calving rates in freshwater are many times smaller than in tidewater, and show that this is so even when the calving front is afloat and intensely crevassed.

3. Unlike tidewater glaciers, at which the non-calving/calving transition typically leads to fast recession without delay, lacustrine glacier termini frequently undergo a phase of downwasting and narrowing prior to the onset of rapid terminus retreat. At Glaciar Nef, this phase lasted >50 years. In common with many previous studies of calving glaciers, the 20th-century fluctuation history of Glaciar Nef shows that dynamic and topographic controls can partially decouple glacier-terminus behaviour from the climatic signal over decadal time-scales.

4. Available information from lacustrine calving glaciers

https://doi.org/10.3189/172756501781832403 Published online by Cambridge University Press

shows that in terms of stability, dynamics and climatic sensitivity they form a population distinct from both tidewater glaciers and non-calving glaciers.

ACKNOWLEDGEMENTS

This research was made possible by logistical support from Raleigh International. In particular, we thank those Raleigh Venturers who carried the boat, outboard engine and fuel up and down the length of the Río Nef valley, and T. Williams who took a number of useful photographs from an inaccessible vantage point high above the calving front. M. Aniya kindly made his low-level oblique aerial photographs from 1993 and 1995 available to us. N. Hulton made useful comments on the model. Funding for the fieldwork was provided by the Carnegie Trust for the Universities of Scotland (to C.W.), Coventry University (to S.H.) and the Royal Society (to V.W.). Permission to carry out research in Parque Nacional San Rafael was kindly granted by CONAF (the Chilean Corporación Nacional Forestal). Perceptive input from K. van der Veen, G. K. C. Clarke, R. Naruse and an anonymous referee substantially improved the manuscript.

REFERENCES

Alley, R. B. 1991. Sedimentary processes may cause fluctuations of tidewater glaciers. *Ann. Glaciol.*, **15**, 119–124.

Aniya, M. 1988. Glacier inventory for the Northern Patagonia Icefield, Chile, and variations 1944/45 to 1985/86. *Arct. Alp. Res.*, **20**(2), 179–187.

Aniya, M. 1992. Glacier variation in the Northern Patagonia Icefield, Chile, between 1985/86 and 1990/91. *Bull. Glacier Res.* 10, 83–90.

Aniya, M. 1999. Recent glacier variations of the Hielo Patagónicos, South America, and their contribution to sea level change. *Arct. Antarct. Alp. Res.*, **31**(2), 144–152.

Aniya, M. and H. Enomoto. 1986. Glacier variations and their causes in the Northern Patagonia Icefield, Chile, since 1944. *Arct. Alp. Res.*, **18**(3), 307–316.

Aniya, M. and Y. Wakao. 1997. Glacier variations of Hielo Patagónico Norte, Chile, between 1944/45 and 1995/96. *Bull. Glacier Res.* 15, 11–18.

Aniya, M., H. Sato, R. Naruse, P. Skvarca and G. Casassa. 1996. The use of satellite and airborne imagery to inventory outlet glaciers of the Southern Patagonia Icefield, South America. *Photogramm. Eng. Remote Sensing*, **62**(12), 1361–1369.

Aniya, M., S. Park, R. Naruse, P. Skvarca and G. Casassa. 2000. Variations of some Patagonian glaciers, South America, using RADARSAT and Landsat images. *Science Reports of the Institute of Geoscience A21, University of Tsukuba, Japan*, 23–38.

Brown, C. S., M. F. Meier and A. Post. 1982. Calving speed of Alaska tidewater glaciers, with application to Columbia Glacier. *U.S. Geol. Surv. Prof. Pap.* 1258-C.

Casassa, G. 1987. Ice thickness deduced from gravity anomalies on Soler Glacier, Nef Glacier and the Northern Patagonia Icefield. *Bull. Glacier Res.* 4, 43–57.

Derbyshire, E. 1974. The bathymetry of Jökulsárlón, southeast Iceland. *Geogr. J.*, **140**, 269–273.

Escobar, F., F. Vidal, C. Garín and R. Naruse. 1992. Water balance in the Patagonia icefield. *In* Naruse, R. and M. Aniya, *eds. Glaciological researches in Patagonia, 1990.* Nagoya, Japanese Society of Snow and Ice. Data Center for Glacier Research, 109–119.

Forster, R. R., E. Rignot, B. L. Isacks and K. C. Jezek. 1999. Interferometric radar observations of Glaciares Europa and Penguin, Hielo Patagónico Sur, Chile. *J. Glaciol.*, **45**(150), 325–337.

Funk, M. and H. Röthlisberger. 1989. Forecasting the effects of a planned reservoir which will partially flood the tongue of Unteraargletscher in Switzerland. *Ann. Glaciol.*, **13**, 76–81.

Gagnon, R. E. and P. H. Gammon. 1995. Characterization and flexural strength of iceberg and glacier ice. *J. Glaciol.*, **41**(137), 103–111.

Hanson, B. and R. LeB. Hooke. 2000. Glacier calving: a numerical model of forces in the calving-speed/water-depth relation. *J. Glaciol.*, **46**(153), 188–196.

Harrison, S. and V. Winchester. 1998. Historical fluctuations of the Gualas and Reicher Glaciers, North Patagonian Icefield, Chile. *Holocene*, **8**(4), 481–485.

Harrison, S., V. Winchester and C. R. Warren. In press. Glacier fluctuations. *In* Cook, J., S. Beer, J. Davenport, D. Galloway and S. Harrison, *eds. The Laguna San Rafael National Park, Chile: the natural history of a Patagonian wilderness.* London, Intercept Press.

Hochstein, M. P., M. I. Watson, B. Malengreau, D. C. Nobes and I. Owens. 1998. Rapid melting of the terminal section of the Hooker Glacier (Mt Cook National Park, New Zealand). *N.Z. J. Geol. Geophys.*, **41**(3), 203–218.

Holdsworth, G. 1973. Ice calving into the proglacial Generator Lake, Baffin Island, N.W.T., Canada. *J. Glaciol.*, **12**(65), 235–250.

Hooke, R. LeB., T. Laumann and M. I. Kennett. 1989. Austdalsbreen, Norway: expected reaction to a 40 m increase in water level in the lake into which the glacier calves. *Cold Reg. Sci. Technol.*, **17**(2), 113–126.

Howarth, P. J. and R. J. Price. 1969. The proglacial lakes of Breiðamerkurjökull and Fláarjökull, Iceland. *Geogr. J.*, **135**(4), 573–581.

Hunter, L. E. and R. D. Powell. 1998. Ice foot development at temperate tidewater margins in Alaska. *Geophys. Res. Lett.*, **25**(11), 1923–1926.

Kennett, M., T. Laumann and B. Kjöllmoen. 1997. Predicted response of the calving glacier Svartisheibreen, Norway, and outbursts from it, to future changes in climate and lake level. *Ann. Glaciol.*, **24**, 16–20.

Kirkbride, M. P. 1993. The temporal significance of transitions from melting to calving termini at glaciers in the central Southern Alps of New Zealand. *Holocene*, **3**(3), 232–240.

Kirkbride, M. P. and C. R. Warren. 1997. Calving processes at a grounded ice cliff. *Ann. Glaciol.*, **24**, 116–121.

Kirkbride, M. P. and C. R. Warren. 1999. Tasman Glacier, New Zealand: 20th-century thinning and predicted calving retreat. *Global and Planetary Change*, **22**(1–4), 11–28.

Kobayashi, S. and T. Saito. 1985. Heat balance on Soler glacier. *In* Nakajima, C., *ed. Glaciological studies in Patagonia Northern Icefield, 1983–1984.* Nagoya, Japanese Society of Snow and Ice. Data Center for Glacier Research, 46–51.

Krimmel, R. M. 1997. Documentation of the retreat of Columbia Glacier, Alaska. *Byrd Polar Res. Cent. Rep.* 15, 105–108.

Lingle, C. S., A. Post, U. C. Herzfeld, B. F. Molnia, R. M. Krimmel and J. J. Roush. 1993. Correspondence. Bering Glacier surge and iceberg-calving mechanism at Vitus Lake, Alaska, U.S.A. *J. Glaciol.*, **39**(133), 722–727.

Lliboutry, L. 1998. Glaciers of South America — glaciers of Chile and Argentina. *U.S. Geol. Surv. Prof. Pap.* 1386-I, I109–I206.

Luckman, B. H. and R. Villalba. 2001. Assessing synchroneity of glacier fluctuations in the western cordillera of the Americas during the last millennium. *In* Markgraf, V., *ed. Interhemispheric climate linkages.* London, Academic Press, 119–140.

Matsuoka, K. and R. Naruse. 1999. Mass balance features derived from a firn core at Hielo Patagónico Norte, South America. *Arct. Antarct. Alp. Res.*, **31**(4), 333–340.

Meier, M. F. 1997. The iceberg discharge process: observations and inferences drawn from the study of Columbia Glacier. *Byrd Polar Res. Cent. Rep.* 15, 109–114.

Meier, M. F. and A. Post. 1987. Fast tidewater glaciers. *J. Geophys. Res.*, **92**(B9), 9051–9058.

Meier, M. *and 9 others.* 1994. Mechanical and hydrologic basis for the rapid motion of a large tidewater glacier. 1. Observations. *J. Geophys. Res.*, **99**(B8), 15,219–15,229.

Mercer, J. H. 1961. The response of fjord glaciers to changes in the firn limit. *J. Glaciol.*, **3**(29), 850–858.

Michel, R. and E. Rignot. 1999. Flow of Glaciar Moreno, Argentina, from repeat-pass Shuttle Imaging Radar images: comparison of the phase correlation method with radar interferometry. *J. Glaciol.*, **45**(149), 93–100.

Naruse, R. and P. Skvarca. 2000. Dynamic features of thinning and retreating Glaciar Upsala, a lacustrine calving glacier in southern Patagonia. *Arct. Antarct. Alp. Res.*, **32**(4), 485–491.

Naruse, R., M. Aniya, P. Skvarca and G. Casassa. 1995a. Recent variations of calving glaciers in Patagonia, South America, revealed by ground surveys, satellite-data analyses and numerical experiments. *Ann. Glaciol.*, **21**, 297–303.

Naruse, R., P. Skvarca, K. Satow, Y. Takeuchi and K. Nishida. 1995b. Thickness change and short-term flow variation of Moreno Glacier, Patagonia. *Bull. Glacier Res.* 13, 21–28.

Naruse, R., P. Skvarca and Y. Takeuchi. 1997. Thinning and retreat of Glaciar Upsala, and an estimate of annual ablation changes in southern Patagonia. *Ann. Glaciol.*, **24**, 38–42.

Pelto, M. S. and C. R. Warren. 1991. Relationship between tidewater glacier calving velocity and water depth at the calving front. *Ann. Glaciol.*, **15**, 115–118.

Powell, R. D. 1990. Advance of glacial tidewater fronts in Glacier Bay, Alaska. *In* Milner, A. M. and J. D. Wood, Jr, *eds. Proceedings of the Second Glacier Bay Science Symposium, 1988.* Anchorage, AK, U.S. Department of the Interior. National Park Service, 67–73.

Powell, R. D. 1991. Grounding-line systems as second-order controls on fluctuations of tidewater termini of temperate glaciers. *In* Anderson, J. B. and G. M. Ashley, *eds. Glacial marine sedimentation; paleoclimatic significance.* Boulder, CO,

https://doi.org/10.3189/172756501781832403 Published online by Cambridge University Press

Geological Society of America, 75–93. (GSA Special Paper 261.)
Qamar, A. 1988. Calving icebergs: a source of low-frequency seismic signals from Columbia Glacier, Alaska. *J. Geophys. Res.*, **93**(B6), 6615–6623.
Reeh, N. 1968. On the calving of ice from floating glaciers and ice shelves. *J. Glaciol.*, **7**(50), 215–232.
Reeh, N. 1994. Calving from Greenland glaciers: observations, balance estimates of calving rates, calving laws. *In* Reeh, N., *ed. Report of a Workshop on "The Calving Rate of the West Greenland Glaciers in Response to Climate Change", Copenhagen, 13–15 September 1993.* Copenhagen, Danish Polar Center, 85–102.
Reid, J. R. and E. Callender. 1965. Origin of debris-covered icebergs and mode of flow of ice into "Miller Lake", Martin River Glacier, Alaska. *J. Glaciol.*, **5**(40), 497–503.
Rignot, E., R. Forster and B. Isacks. 1996a. Interferometric radar observations of Glaciar San Rafael, Chile. *J. Glaciol.*, **42**(141), 279–291. (Erratum: **42**(142), p. 591.)
Rignot, E., R. Forster and B. Isacks. 1996b. Mapping of glacial motion and surface topography of Hielo Patagónico Norte, Chile, using satellite SAR L-band interferometry data. *Ann. Glaciol.*, **23**, 209–216.
Rist, M. A., P. R. Sammonds, S. A. F. Murrell, P. G. Meredith, H. Oerter and C. S. M. Doake. 1996. Experimental fracture and mechanical properties of Antarctic ice: preliminary results. *Ann. Glaciol.*, **23**, 284–292.
Rosenblüth, B., G. Casassa and H. Fuenzalida. 1995. Recent climatic changes in western Patagonia. *Bull. Glacier Res.* 13, 127–132.
Rott, H., M. Stuefer, A. Siegel, P. Skvarca and A. Eckstaller. 1998. Mass fluxes and dynamics of Moreno Glacier, Southern Patagonia Icefield. *Geophys. Res. Lett.*, **25**(9), 1407–1410.
Skvarca, P. and R. Naruse. 1997. Dynamic behavior of Glaciar Perito Moreno, southern Patagonia. *Ann. Glaciol.*, **24**, 268–271.
Skvarca, P., M. Stuefer and H. Rott. 1999. Temporal changes of Glaciar Mayo and Laguna Escondida, southern Patagonia, detected by remote sensing data. *Global and Planetary Change*, **22**(1–4), 245–253.
Theakstone, W. H. 1989. Further catastrophic break-up of a calving glacier: observations at Austerdalsisen, Svartisen, Norway, 1983–87. *Geogr. Ann.*, **71A**(3–4), 245–253.
Theakstone, W. H. and N. T. Knudsen. 1986. Recent changes of a calving glacier, Austerdalsisen, Svartisen, Norway. *Geogr. Ann.*, **68A**(4), 303–316.
Van der Veen, C. J. 1996. Tidewater calving. *J. Glaciol.*, **42**(141), 375–385.
Van der Veen, C. J., *ed.* 1997. Calving glaciers: report of a Workshop, February 28–March 2, 1997, Columbus, OH. *Byrd Polar Res. Cent. Rep.* 15.
Vaughan, D. G. 1993. Relating the occurrence of crevasses to surface strain rates. *J. Glaciol.*, **39**(132), 255–266.
Venteris, E. R. 1999. Rapid tidewater glacier retreat: a comparison between Columbia Glacier, Alaska and Patagonian calving glaciers. *Global and Planetary Change*, **22**(1–4), 131–138.
Venteris, E. R., I. M. Whillans and C. J. van der Veen. 1997. Effect of extension rate on terminus position, Columbia Glacier, Alaska, U.S.A. *Ann. Glaciol.*, **24**, 49–53.
Wada, Y. and M. Aniya. 1995. Glacier variations in the northern Patagonia Icefield between 1990/91 and 1993/94. *Bull. Glacier Res.* 13, 111–119.
Warren, C. R. 1991. Terminal environment, topographic control and fluctuations of West Greenland glaciers. *Boreas*, **20**(1), 1–15.
Warren, C. R. 1994. Freshwater calving and anomalous glacier oscillations: recent behaviour of Moreno and Ameghino Glaciers, Patagonia. *Holocene*, **4**(4), 422–429.
Warren, C. R. 1999. Calving speed in freshwater at Glaciar Ameghino, Patagonia. *Z. Gletscherkd. Glazialgeol.*, **35**(1), 21–34.
Warren, C. R. In press. Glacier calving dynamics. *In* Cook, J., S. Beer, J. Davenport, D. Galloway and S. Harrison, *eds. The Laguna San Rafael National Park, Chile: the natural history of a Patagonian wilderness*. London, Intercept.
Warren, C. and M. Aniya. 1999. The calving glaciers of southern South America. *Global and Planetary Change*, **22**(1–4), 59–77.
Warren, C. R. and M. P. Kirkbride. 1998. Temperature and bathymetry of ice-contact lakes in Mount Cook National Park, New Zealand. *N.Z. J. Geol. Geophys.*, **41**(2), 133–143.
Warren, C. R. and D. E. Sugden. 1993. The Patagonian icefields: a glaciological review. *Arct. Alp. Res.*, **25**(4), 316–331.
Warren, C. R., D. E. Sugden and C. M. Clapperton. 1995a. Asynchronous response of Patagonian glaciers to historic climate change. *Quaternary of South America and the Antarctic Peninsula*, **9**, 85–103.
Warren, C. R., N. F. Glasser, S. Harrison, V. Winchester, A. R. Kerr and A. Rivera. 1995b. Characteristics of tide-water calving at Glaciar San Rafael, Chile. *J. Glaciol.*, **41**(138), 273–289; Erratum: **41**(139), p. 281.
Warren, C. R., D. R. Greene and N. F. Glasser. 1995c. Glaciar Upsala, Patagonia: rapid calving retreat in fresh water. *Ann. Glaciol.*, **21**, 311–316.
Warren, C. R., A. Rivera and A. Post. 1997. Greatest Holocene advance of Glaciar Pio XI, Chilean Patagonia: possible causes. *Ann. Glaciol.*, **24**, 11–15.
Winchester, V. and S. Harrison. 1996. Recent oscillations of the San Quintin and San Rafael Glaciers, Patagonian Chile. *Geogr. Ann.*, **78A**(1), 35–49.
Winchester, V., S. Harrison, R. Washington and C. R. Warren. 1999. Austral summer of 1998: observations on El Niño and the North Patagonian Icefield. *Weather*, **54**(9), 287–293.
Winchester, V., S. Harrison and C. R. Warren. In press. Recent retreat of Glaciar Nef, Chilean Patagonia, dated by lichenometry and dendrochronology. *Arct. Antarct. Alp. Res.*
Yoshida, K. 1981. Estudio geologicos del curso superior del Rio Baker, Aisen, Chile. (Ph.D. thesis, Universidad de Chile, Santiago.)

MS received 4 October 1999 and accepted in revised form 21 December 2000